Servo Performance Enhancement of Motion System using Quantized Output Reconstruction Approach

Hongzhong Zhu, Hiroshi Fujimoto (The University of Tokyo)
Toshiharu Sugie (Kyoto University)

Abstract
Optical encoders are extensively used for position measurements in motion control systems. The inherent quantization feature of the optical encoders limits the performance in many high accuracy control applications. In this paper, a new approach is presented to reconstruct the position signals of motion system in the case that low resolution encoders are applied for position measurements. By fitting the quantized measurements with polynomials in a moving horizon manner, a reconstruction of position is obtained via solving a convex optimization problem. Some constraint conditions are also taken into account for obtaining accurate smooth reconstruction. The effectiveness of the proposed approach is demonstrated by simulations and experiments using a high-precision linear stage.

Key words: quantization, optical encoder, motion control, polynomial fitting approach, convex optimization

1. Introduction

Quantization is an inherent feature in motion systems whose position signals are measured by optical encoder. In some cases, the quantization error is substantially small compared to system noise or the desired position accuracy. However, this is not always the case since the control performance is stringently required in storage devices, NC machine tools, industrial robots, and so on. When the quantized measurement is used as the control signal directly, the quantization error will degrade the control accuracy or cause self-excited oscillations. Therefore, understanding and suppressing the quantization effects have attracted a great deal of attention [(1)(2)].

A lot of literature can be found on reducing the quantization effects based on system model. These methods usually exploit observer techniques [(3)(4)] or Kalman filters [(5)(6)], and have the potential to achieve precise state estimation since they can take advantage of the system information. However, it should be noticed that most of the observer-based methods disregard the effects caused by the input disturbance or the measurement noise, or both of them. This may be difficult to apply in many practical situations. On the other hand, the methods based on Kalman filters usually make the assumption that the quantization error is Gaussian noise. In fact, quantization error behaves as highly colored noise and these methods are not always effective.

Several other approaches devote efforts to reconstruct the output based on curve fitting techniques. The idea is usually based on the assumption that the system output can locally be approximated by polynomials. The other variables of the system, such as velocity and acceleration, can therefore be estimated by calculating the first and second order derivative of the polynomials [(7)(8)]. The methods can achieve a smooth and precise reconstruction signal only if the quantization step is small and low-order polynomial is applied.

Since the model-based methods share the feature of providing good estimation performance and polynomial fitting methods can achieve a smooth reconstruction signal, the purpose of this paper is to propose a new method by combining them together. More concretely, we try to obtain more precise information on the current output from a series of past quantized measurement by taking account of the plant dynamics. At the same time, a polynomial fitting approach is exploited in order to achieve smooth system output estimate/reconstruction. A similar approach is proposed for estimating the velocity information from the quantized measurements [(9)]. However, the non-zero-mean disturbance, such as the mechanical friction existing in all motion systems, is not taken into account. In this paper, we also cope with this problem and try to make the reconstruction approach more applicable.

This paper is organized as follows. In Section 2, the system model is introduced, and the problem setting is described. Section 3 presents the moving horizon polynomial fitting approach and analyzes the reconstruction error. Sections 4 and 5 demonstrate the effectiveness of the proposed approach by experiments using a high-precision positioning system. The conclusions are summarized in Section 6.

2. System Description

Consider the discrete-time linear time-invariant SISO system with quantized output given by

$$\boldsymbol{x}[k+1] = \boldsymbol{A}\boldsymbol{x}[k] + \boldsymbol{B}u[k] + \boldsymbol{F}w[k], \quad \boldsymbol{x}[0] = 0, \cdots (1)$$

$$y[k] = \boldsymbol{C}\boldsymbol{x}[k], \cdots (2)$$

$$y_v[k] = y[k] + v[k], \cdots (3)$$

$$y_q[k] = \boldsymbol{Q}(y_v[k]), \cdots (4)$$

where $\boldsymbol{A} \in \mathbb{R}^{n\times n}, \boldsymbol{B} \in \mathbb{R}^{n\times 1}, \boldsymbol{F} \in \mathbb{R}^{n\times 1}, \boldsymbol{C} \in \mathbb{R}^{1\times n}$ are constant system matrices, and $(\boldsymbol{C}, \boldsymbol{A})$ is observable. $\boldsymbol{x} \in \mathbb{R}^n$, $y \in \mathbb{R}$, $y_v \in \mathbb{R}$ and $y_q \in \mathbb{R}$ are the plant state, the system output, the corrupted output and the quantized output, respectively. $v \in \mathbb{R}$, $w \in \mathbb{R}$ are the measurement noise and

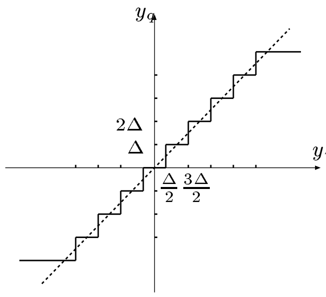

Fig. 1. Quantization characteristic. Δ is the quantization step.

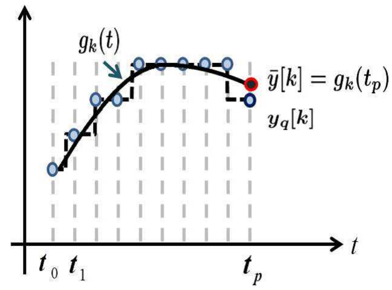

Fig. 2. Fitting strategy.

the input disturbance. v is assumed to be zero mean and bounded by $\|v\|_\infty \leq \delta$ with known δ. The function $\boldsymbol{Q}(\cdot)$ represents the uniform quantizer defined by

$$\boldsymbol{Q}(y_v) = i \cdot \Delta, \quad y_v \in ((i-0.5)\Delta\ ,\ (i+0.5)\Delta], \cdots (5)$$

where $i \in Z$, $\Delta > 0$ denotes the quantization step. The quantization range is assumed to be infinite. The relationship between y_v and y_q is shown in Fig. 1.

Due to the measurement noise v, the difference between the system output y and the measured quantized output y_q, denoted as $\xi := y - y_q$, is bounded by

$$|\xi| \leq \frac{\Delta}{2} + \delta. \cdots (6)$$

In a motion control system where an optical encoder is applied for measuring the position information, limit cycle oscillation would be caused by the quantized measurements. Moreover, the system input may exhibit wild behavior when the controller is high-gain or has derivative term. This motivates us to smoothly reconstruct the system output y from the quantized measurements. Since the true system output y should be smooth and band limited due to the plant dynamics, it is possible to get more precise information on current position $y[k]$ from the past quantized measurement series $y_q[i]$ $(i \leq k)$. In the next section, we improve the moving horizon polynomial fitting approach [9] by applying the extended observer to cope with the non-zero-mean input disturbance.

3. Moving Horizon Polynomial Fitting Approach

In this section, a moving horizon polynomial fitting approach [9] is introduced to reconstruct the system output. Firstly, the quantized measurements are locally fitted by a polynomial via the ℓ_1-norm regularization. Then, the moving horizon manner is applied for the real-time output reconstruction. Finally, several constraint conditions are derived to improve the fitting accuracy by taking into account the quantization feature and the model information.

3.1 Polynomial Fitting Formulation At time instant k, a polynomial for fitting the latest $p+1$ quantized measurements $(\{y_q[k-i]\}_{i=0,1,\cdots,p})$ is considered. In order to do so, first, choose the time interval $[a\ \ b]$ in advance, and introduce the virtual time indices $\{t_i\}_{i=0,1,\cdots,p}$, which are defined by

$$t_0 = a, t_1 = a+h, \cdots, t_i = a+ih, \cdots, t_p = b,$$

where $h = (b-a)/p$, to equally divide $[a\ \ b]$. Then the data $(t_i, y_q[k-p+i])_{i=0,1,\cdots,p}$ are fitted in Euclidean space with a polynomial:

$$g_k(t) = \alpha_0 + \alpha_1 t + \alpha_2 t^2 + \cdots + \alpha_m t^m,\ t \in [a\ \ b] \cdot\cdot (7)$$

where $\alpha_0,\ \alpha_1,\ \cdots\ \alpha_m$ are the coefficients, and m is the degree of the polynomial. Without loss of generality, the degree m is set as $m \leq p+1$. The fitting problem is formulated by

$$\underset{\boldsymbol{\alpha}}{\text{minimize}} : \left\| \begin{bmatrix} g_k(t_0) - y_q[k-p] \\ \vdots \\ g_k(t_i) - y_q[k-p+1] \\ \vdots \\ g_k(t_p) - y_q[k] \end{bmatrix} \right\|_2, \cdots (8)$$

with variables $\boldsymbol{\alpha} := [\alpha_0\ \alpha_1\ \cdots\ \alpha_m]^T$. Fig. 2 demonstrates the fitting strategy. The problem (8) can be expressed as

$$\underset{\boldsymbol{\alpha}}{\text{minimize}} : \quad \|\boldsymbol{T}\boldsymbol{\alpha} - \boldsymbol{\beta}\|_2, \cdots (9)$$

with variable $\boldsymbol{\alpha}$, where

$$\boldsymbol{T} = \begin{bmatrix} 1 & t_0 & t_0^2 & \cdots & t_0^m \\ 1 & t_1 & t_1^2 & \cdots & t_1^m \\ \vdots & \vdots & \vdots & \ddots & \vdots \\ 1 & t_i & t_i^2 & \cdots & t_i^m \\ \vdots & \vdots & \vdots & \ddots & \vdots \\ 1 & t_p & t_p^2 & \cdots & t_p^m \end{bmatrix},\ \boldsymbol{\beta} = \begin{bmatrix} y_q[k-p] \\ y_q[k-p+1] \\ \vdots \\ y_q[k-p+i] \\ \vdots \\ y_q[k] \end{bmatrix}.$$

The time indices $\{t_i\}_{i=0,1,\cdots,p}$ is normally chosen as the real time instants. However, in this case, the resulting matrix $\boldsymbol{T}$ would become ill-condition and the fitting accuracy cannot be guaranteed, because the calculation accuracy for solving the $\boldsymbol{\alpha}$ may be degraded. Referring to the *Theorem 3.1* in [12], a symmetric interval with respect to the origin is necessarily to minimize the condition number of $\boldsymbol{T}$. Therefore, $[a\ \ b]$ is chosen as $[-1\ \ 1]$ in this study without loss of generality.

Once the polynomial is calculated, the quantity $\bar{y}[k]$ given by

$$\bar{y}[k] := g_k(t_0) = \alpha_0 + \alpha_1 t_p + \alpha_2 t_p^2 + \cdots + \alpha_m t_p^m, \cdot (10)$$

is regarded as the approximation of the system output $y[k]$. This is a common least square fitting method which is widely used [7]. However, it is usually difficult to choose an appropriate m for the polynomial to fit the quantized measurements since high-degree polynomial would lead to erroneous

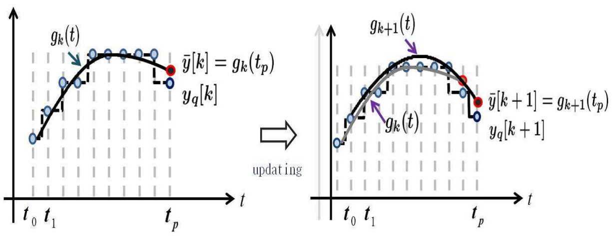

Fig. 3. Updating strategy. A new polynomial should be calculated when the time instant is updated.

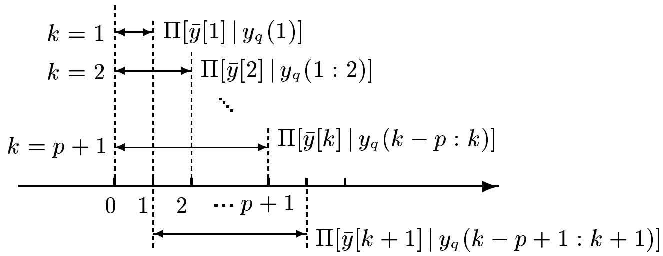

Fig. 4. Moving horizon output reconstruction strategy.

fitting. For instance, it may yield overshoot or wild oscillations [10]. Therefore, a compromise that setting a proper high dimension m for the polynomial in advance and taking some heuristics to automatically reduce the dimension is necessary. Since ℓ_1-norm puts relatively larger emphasis on small residuals and can get a sparse solution [11], the following ℓ_1-norm regularization method is exploited to reduce the number of non-zero coefficients. The polynomial fitting problem is formed by

$$\underset{\boldsymbol{\alpha}}{\text{minimize}}: \quad \|\boldsymbol{T}\boldsymbol{\alpha} - \boldsymbol{\beta}\|_2^2 + \eta\|\boldsymbol{\alpha}\|_1, \cdots\cdots\cdots\cdots (11)$$

with variables $\boldsymbol{\alpha} \in \mathbb{R}^{m+1}$, where η is the weighting factor.

3.2 Moving Horizon Approach In this subsection, a moving horizon approach is introduced for updating the reconstruction. Suppose that the time instant k is updated, say, from k to $k+1$, a new quantized measurement $y_q[k+1]$ is sampled. Fig. 3 shows the updating strategy. A new polynomial $g_{k+1}(t)$ is thus determined to fit the data $\{y_q[k-p+1], y_q[k-p+2], \cdots, y_q[k+1]\}$, and the approximate value of the system output $y[k+1]$ is calculated by

$$\bar{y}[k+1] = g_{k+1}(t_0).$$

This procedure is denoted as $\boldsymbol{\Pi}[\bar{y}[k+1] \mid y_q(k-p+1:k+1)]$. In the case of $k \le p$, $y_q[k-i]$ $(i = k, k+1, \cdots, p)$ is set as $y_q[k-i] := 0$. The calculation procedure in this case is denoted by $\boldsymbol{\Pi}[\bar{y}[k] \mid y_q(1:k)]$ because the quantized measurements $y_q[i]_{i=1,\cdots,k}$ are only used. The approximation signal $\bar{y}$ of true system output y is obtained by successively repeating this procedure. Fig. 4 demonstrates the moving horizon output approximation strategy.

3.3 Constraint Conditions In order to improve the approximate accuracy and obtain a smooth signal $\bar{y}$, the model information, which will be exploited to form several constraint conditions, is taken into account in the following. As described in Section 2, the system output relative to the quantized output is always bounded by (6). Therefore, the approximate value $\bar{y}(k)$ should also be bounded as same as (6). So the following constraint

$$|g_k(t_0) - y_q[k]| \le \frac{\Delta}{2} + \delta, \cdots\cdots\cdots\cdots\cdots\cdots (12)$$

can be added to the problem (11).

In [9], the following two conditions are added to the problem (11) to obtain a smooth reconstruction.

$$g_k(t_1) = \hat{y}[k-1], \cdots\cdots\cdots\cdots\cdots\cdots (13)$$

$$\dot{g}_k(t_1) = \frac{1}{h}(\hat{y}[k] - \hat{y}[k-1]), \cdots\cdots\cdots\cdots (14)$$

where $\hat{y}$ is the estimated output of the following observer

$$\hat{\boldsymbol{x}}[k+1] = \boldsymbol{A}\hat{\boldsymbol{x}}[k] + \boldsymbol{B}u[k] + \boldsymbol{L}(\bar{y}[k] - \hat{y}[k]), \cdots\cdots (15)$$

$$\hat{y}[k] = \boldsymbol{C}\hat{\boldsymbol{x}}[k]. \cdots\cdots\cdots\cdots\cdots\cdots (16)$$

$\boldsymbol{L} \in \mathbb{R}^{n\times 1}$ is the observer gain. Since the observer (15) is sensitive to input disturbance including mechanical friction, the extended observer of the system (1) (2) is exploited to estimate the disturbance w. Define the extended state as $\tilde{\boldsymbol{x}} = [x \ w]^T$, the observer is expressed as

$$\tilde{\boldsymbol{x}}[k+1] = \boldsymbol{A}_e\tilde{\boldsymbol{x}}[k] + \boldsymbol{B}_e u[k] + \boldsymbol{L}_e(\bar{y}[k] - \tilde{y}[k]), \cdots (17)$$

$$\tilde{y}[k] = \boldsymbol{C}_e\tilde{\boldsymbol{x}}[k], \cdots\cdots\cdots\cdots\cdots\cdots (18)$$

where

$$\boldsymbol{A}_e = \begin{bmatrix} \boldsymbol{A} & \boldsymbol{F} \\ \boldsymbol{0} & 0 \end{bmatrix}, \ \boldsymbol{B}_e = \begin{bmatrix} \boldsymbol{B} \\ 0 \end{bmatrix}, \ \boldsymbol{C}_e = \begin{bmatrix} \boldsymbol{C} & 0 \end{bmatrix}.$$

The gain $\boldsymbol{L}_e \in \mathbb{R}^{(n+1)\times 1}$ in (17) is designed to stabilize $\boldsymbol{A}_e - \boldsymbol{L}_e\boldsymbol{C}_e$. The conditions (13) (14) can be replaced by

$$g_k(t_1) = \tilde{y}[k-1], \cdots\cdots\cdots\cdots\cdots\cdots (19)$$

$$\dot{g}_k(t_1) = \frac{1}{h}(\tilde{y}[k] - \tilde{y}[k-1]), \cdots\cdots\cdots\cdots (20)$$

3.4 system output Reconstruction The quantized output reconstruction algorithm is summarized as follows:

Algorithm: State estimation

(1) ***Choose*** *proper values for* p, m, η; *set initial value* $\boldsymbol{\beta} = 0$, *assign the values for* Δ, δ;

(2) ***repeat***

(a) *Sample the position measurement* $y_q[k]$, *update the vector* $\boldsymbol{\beta}$;

(b) *solve the problem*

$$\underset{\boldsymbol{\alpha}}{\text{minimize}}: \quad \|\boldsymbol{T}\boldsymbol{\alpha} - \boldsymbol{\beta}\|_2^2 + \eta\|\boldsymbol{\alpha}\|_1 \quad \cdots\cdots (21)$$

subject to : (12), (19), (20);

(c) *calculate* $\bar{\theta}[k]$, $\tilde{\boldsymbol{x}}[k]$ *by (10), (19) and (20)*;

(d) set $k \leftarrow k+1$.

The optimization problem (21) is a convex optimization problem and can be solved if the problem is feasible. Note that the three constraint conditions are independent with each other, so the problem is feasible if the polynomial (7) has a dimension not less than 3 $(m+1 \ge 3)$.

4. Experiments

This section demonstrates the application of the improved moving horizon polynomial fitting approach to a

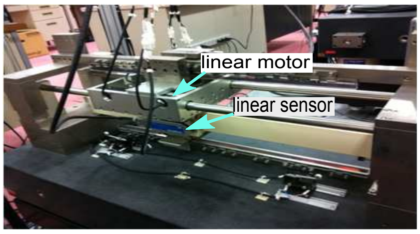

Fig. 5. Experimental setup.

Table 1. Parameters of the stage

Inductance L	15.5×10^{-3}	H
Resistance R	20.5	Ω
Mass M	14.5	kg
Viscosity B	24	N/(m/s)
Thrust coefficient K_t	26.5	N/A
Bach-EMF constant K_e	16	V/(m/s)

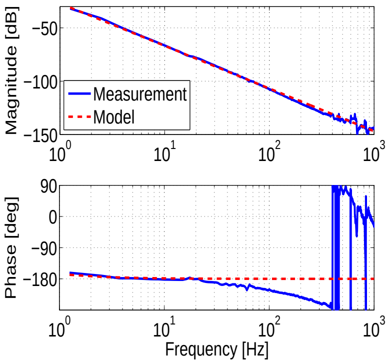

Fig. 6. Frequency characteristics.

high-precision stage. Fig. 5 shows the experimental setup, whose parameters are shown in Table. 1. The stage is driven by linear motors located at the both sides of the carrier. The control input is the motor current and the output is the position. DSP(TMS320C6713, 225MHz) is used as the processor to implement the controllers and the fitting approach. A linear encoder with a resolution of 1nm is exploited for position measurement. Fig. 6 shows the frequency characteristics of the Stage. The nominal model is expressed as

$$P(s) = \frac{26.5}{s(14.7s + 24)}, \cdots\cdots\cdots\cdots (22)$$

where s is the Laplace operator. PTC (perfect tracking controller) [13] is exploited as the feedforward controller and a PID compensator is exploited as the feedback controller. Fig. 7 shows the block diagram of the control system. In order to evaluate the reconstruction accuracy of the proposed approach, a software quantizer is introduced. The signal y from the linear encoder is assumed to be the actual output and the signal y_q from the software quantizer is regarded as the measurement output. The position tracking error and the reconstruction error are defined as

$$e_t = y_d - y, \cdots\cdots\cdots\cdots (23)$$

$$e_r = \bar{y} - y, \cdots\cdots\cdots\cdots (24)$$

respectively. The sampling period is set as $T_s = 5$ ms. A discrete-time state space expression of (22) using zero-order

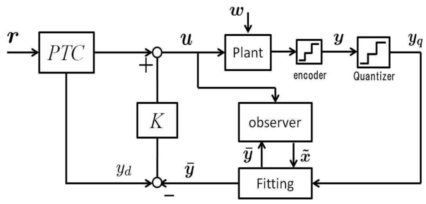

Fig. 7. Block diagram of linear stage control system.

hold method is

$$\boldsymbol{x}[k+1] = \begin{bmatrix} 1 & 0.0050 \\ 0 & -0.9919 \end{bmatrix} \boldsymbol{x}[k] + \begin{bmatrix} 2.247e^{-5} \\ 8.977e^{-3} \end{bmatrix} u[k],$$

$$y[k] = \begin{bmatrix} 1 & 0 \end{bmatrix} x[k].$$

The feedback controller is designed as

$$K = k_p + k_d \frac{s}{0.004s + 1} + k_i \frac{1}{s}, \cdots\cdots\cdots\cdots (25)$$

where $k_p = 2065.6$, $k_i = 34624$, $k_d = 43.45$, the close-loop system obtain the triple roots at $10Hz$. The controller is also discretized with the sampling period $T_s = 5$ ms by tustin transformation.

In these experiments, the input disturbance is also considered to design the extended observer (17). The disturbance matrix $\boldsymbol{F}$ is set as $\boldsymbol{F} = \boldsymbol{B}$. The gain $\boldsymbol{L}_e$ of state estimator is also selected by placing the poles of the observer at [0.5335, 0.6242, 0.7304]. The resulting observer bandwidth is about 20Hz.

The C code of convex optimization problem (21) is generated by CVXGEN [14]. The number of data used for polynomial fitting is set as $p+1 = 15$, and the degree of polynomial is set as $m = 3$. The weight factor η is properly chosen as $\eta = 2e^{-3}$. The quantization step is set as $\Delta = 20\mu$m, δ is set as $2e^{-9}$. For comparison, the low-pass filter

$$F(s) = \frac{1}{1 + 0.002s}, \cdots\cdots\cdots\cdots (26)$$

is also exploited to reduce the effects of the quantized measurements.

In the setup, the position and trajectory reference of the linear stage is given as Fig. 8. The experimental results are shown in Fig. 9, Fig. 10 and Fig. 11. Fig. 9 shows the results in the case that the quantized measurements are used for feedback. Fig. 9(a) shows the comparison of the desired reference y_d and real output y, and Fig. 9(b) shows their difference. It is observed that the high-order vibration is raised not only at the servo state, but also at the steady state. The quantization error is shown in Fig. 9(c). The control input is shown in Fig. 9(d). It is shown that the control input also changed wildly, which is also not good for precise control. Fig. 10 shows the results when the low-pass filter is used. Fig. 10(a) shows the comparison of the desired output and the filtered output. Fig. 10(b) shows the position tracking error. It is observed that the tracking performance is degraded by the time delay introduced by the filter. Fig. 10(c) shows th control input. On the other hand, Fig. 11 shows the results in the case that the proposed fitting approach is applied. Fig. 11(a) shows the comparison of the desired reference, the controlled output y and the reconstructed output. The position tracking error and the reconstructed error

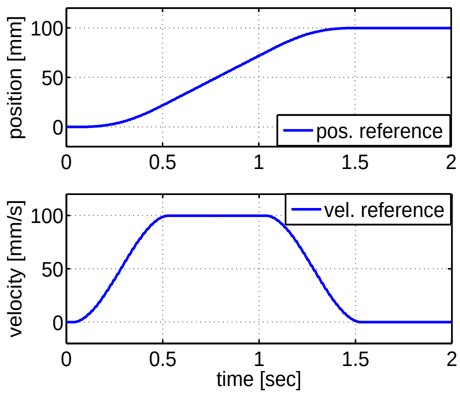

Fig. 8. Trajectory reference.

are shown in Fig. 11(b), (c). It is observed that the reconstruction error is much smaller than the quantization error. Moreover, the high-order vibration is also suppressed, especially at the steady state. Fig. 11(d) shows the control input and the estimated disturbance. It is observed that the control input is smoother compared to Fig. 9(d). Therefore, the effectiveness of the proposed method is verified.

5. Conclusion

In this paper, a method is proposed to reconstruct the output of motion systems with quantized measurements. It exploits the moving horizon polynomial fitting approach with some additional constraints, which takes into account the feature of quantization and the smoothness of the output. The approach is based on the extended observer and the convex optimization technique, and therefore it is computationally tractable. The approach is also applied to a high-precision linear stage with an optical encoder that is low-resolution. The experimental results demonstrate the effectiveness of the proposed method.

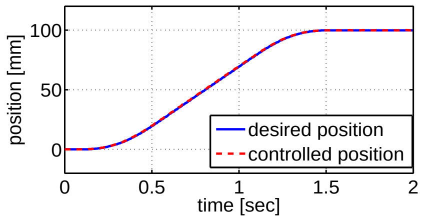

(a)

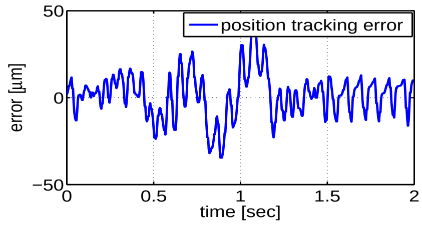

(b)

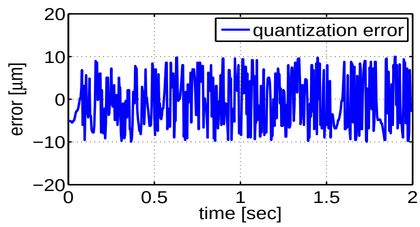

(c)

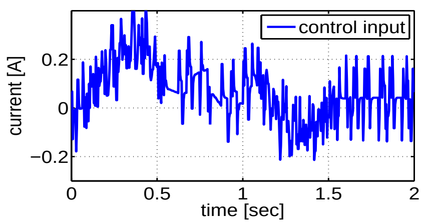

(d)

Fig. 9. Experimental results in the case that the quantized measurements used for feedback. (a) shows the comparison of the desired reference y_d and real output y, (b) shows the position tracking error. (c) shows the quantization error, and (d) shows the control input.

References

(1) J. Sur, and B. E. Paden, State Observer for Linear Time-Invariant Systems With Quantized Output. *Journal of Dynamic Systems, Measurement, and Control*, Vol. 120, pp. 423-426, Sep. 1998.

(2) F. Franklin, J. D. Powell, M. Workman, *Digital Control of Dynamic Systems*, 3rd edition, Addison-Wesley, 1998.

(3) Tod R. Tesch, Robert D. Lorenz, Disturbance Torque and Motion State Estimation with Low-Resolution Position Interfaces Using Heterodyning Observers. *IEEE Transactions on Industrial Applications*, Vol. 44, No. 1, Jan. 2008.

(4) J. Zhang, M. Fu, A Reset State Estimator for Linear Systems to Suppress Sensor Quantization Effects. Proc. 17th IFAC World Congress, pp. 9254-9259, 2008.

(5) D. Luong-Van, M. Tordon, J. Katupitiya, Covariance Profiling for an Adaptive Kalman filter to Suppress Sensor Quantization Effects. *Proceedings 43rd IEEE Conference on Decision and Control*, 2680–2685, Dec. 2004.

(6) P. R. Bélanger, P. Dobrovolny, A. Helmy, X. Zhang, Estimation of Angular Velocity and Acceleration from Shaft-Encoder Measurements, *The International Journal of Robotics Research* Vol. 17, No. 11, pp. 1225-1233, Nov. 1998.

(7) R. H. Brown, S. C. Schneider, and M. G. Mulligan, Analysis of Algorithms for velocity Estimation from Discrete Position Versus Time Data. *IEEE Transactions on Industrial Electronics*, Vol. 39, No. 1, pp. 11-19, Feb. 1992.

(8) R. J. E. Merry, M. J. G. van de Molengraft, M. Steinbuch, Velocity and acceleration estimation for optical incremental encoders. *Mechatronics 20*, pp. 20-26, 2010.

(9) H. Zhu, and T. Sugie, Velocity Estimation of Motion Systems Based on Low-Resolution Encoders, *Trans. of the ASME, Journal of Dynamic Systems, Measurement and Control*, In press.

(10) G. Strang, *Introduction to Applied Mathematics*, Wellesley, Cambridge Press, 1986.

(11) S. Boyd and L. Vandenberghe, *Convex Optimization*, Cambridge University Press, 2004.

(12) W. Gautschi, Optimally Conditioned Vandermonde Matrices. *Numer. Math.*, Vol. 24, pp. 1-12, 1975.

(13) K. Sakata, H. Fujimoto, High Bandwidth Design of Feedback Control System Using Multiple Sensors for High-Precision Stage, *Proc. The 39th SICE Symposium*

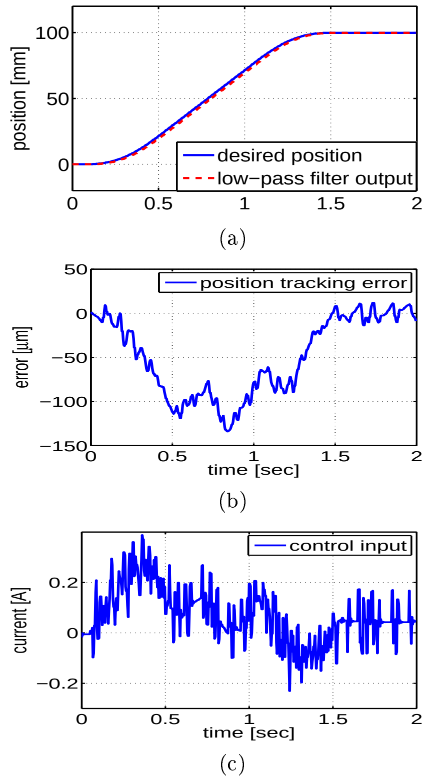

Fig. 10. Experimental results in the case that the low-pass filter is used. (a) shows the comparison of the desired reference y_d and the filtered output. (b) shows the position tracking error. (c) shows the control input.

on Control Theory , pp. 285-290, 2010 (in Japanese).

(14) J. Mattingley, Y. Wang, S. Boyd, Code Generation for moving horizon Control. *Proceedings IEEE Multi-Conference on Systems and Control*, pp. 985-992, Yokohama, Japan, Sep., 2010.

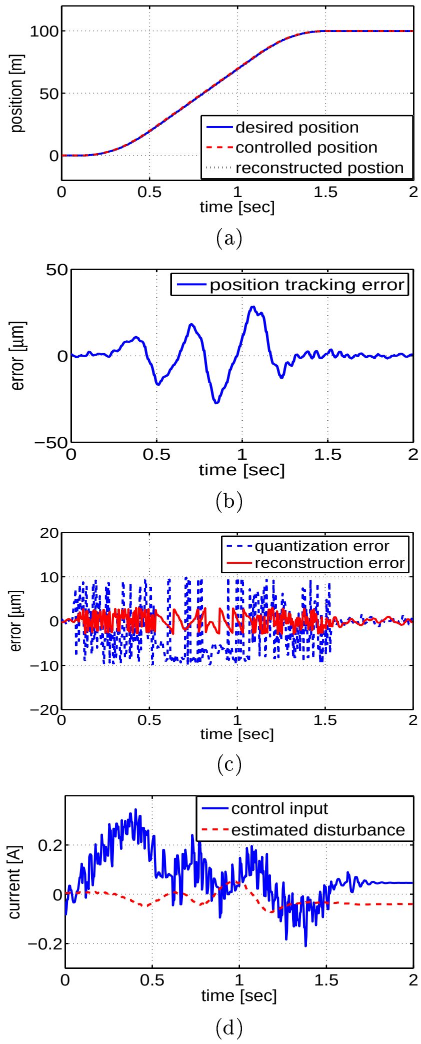

Fig. 11. Experimental results in the case that the quantized measurements is fitted. (a) shows the comparison of the desired reference y_d, real output y and the reconstructed output $\bar{y}$, (b) shows the position tracking error. (c) shows the quantization error and the reconstruction error, and (d) shows the control input and the estimated disturbance.